Journal of Global Positioning Systems (2008)
Vol. 7, No. 2: 133-147

Journal of Global Positioning Systems
2008

QR Implementation of GNSS Centralized Approaches

A. Lannes
CNRS/LSS/[1] (France)

S. Gratton
CNES/OMP/[1] (France)

Abstract. When processing times series of global positioning data, one is led to introduce 'local variables,' which depend on the successive epochs of the time series, and a 'global variable' which remains the same all over these epochs with however possible state transitions from time to time. For example, the latter occur when some satellites appear or disappear. In the period defined by two successive transitions, the problem to be solved in the least-square sense is governed by a linear equation in which the key matrix has an angular block structure. This structure is well suited to recursive QR factorization. The corresponding techniques prove to be very efficient for GNSS data processing and quality control in real-time kinematics. The main objective of this paper is to show how the QR implementation of GNSS centralized approaches combines the advantages of all the methods developed hitherto in this field. The study is conducted by considering the simple case of continuous observations with a local-scale single baseline. The extension to networks is simply outlined.

Keywords. GNSS, DGPS, RTK. PPP. DIA. RAIM. LLL. Undifferential centralized data, reduced difference. Recursive Least Square (RLS). Quality control. Integer ambiguity resolution.

1 Introduction

In the traditional approach to differential GNSS, the satellite error terms are eliminated by forming the so-called single differences (SD). One then gets rid of the receiver error terms by computing, for each receiver to be considered, the corresponding double differences (DD): the discrepancies between the single differences (SD) and one of them taken as reference. Note that a similar situation arises in precise point positioning (PPP) with a single receiver. To handle the SD's in a homogeneous manner, one may equally well consider the discrepancies between the SD's and their mean value. By adopting the terminology introduced by Shi and Han (1992), one may then speak of 'centralized differences' (CD). At first sight, the ambiguities to be raised are then rational numbers (which are not necessarily integers). The GNSS community therefore considered that this idea could not be implemented easily. Fifteen years later, this principle was reintroduced in an independent manner (Lannes 2007a). In the corresponding approach, which referred to the same concept, but with another terminology, that of 'reduced difference' (RD), the difficulty related to rational ambiguities was overcome. The connection with the centralized undifferential method was then clarified (Lannes 2007b, 2008). In particular, it was shown that at any stage of the data assimilation procedure, it was possible to pass from the RD mode to the DD mode, and vice-versa. Shortly, the RD mode is well suited to quality control (see Sects. 6 in Lannes 2007b and 2008), while solving the rational-ambiguity problem amounts to solving a nearest-lattice-point problem of DD type (see Sect. 5.2 in Lannes 2007b).

When processing times series of global positioning data, one is led to introduce 'local variables' u_i which depend on the successive epochs t_i of the time series to be processed, and a 'global variable' v which remains the same all over these epochs with however possible state transitions from time to time. For example, the latter occur when some receiver-satellite signals appear or disappear. In the period defined by two successive transitions, the problem to be solved in the least-square (LS) sense is governed by a system of linear equations of the form

$$\left|\begin{array}{l} A_1u_1 + B_1v = b_1 \\ A_2u_2 + B_2v = b_2 \\ \qquad\vdots \\ A_iu_i + B_iv = b_i \end{array}\right. \tag{1}$$

The definition of the variables u_i and v depends on the GNSS system under consideration. The components of u_i and v are real numbers, some components of v being integers (lying in $\mathbb{Z}$): the integer ambiguities of the problem.

[1] This work was also supported by the CERFACS (France): the European Centre for Research and Advanced Training in Scientific Computation.

In matrix terms, Eq. (1) can be displayed as follows:

$$\begin{bmatrix} A_1 & & & & B_1 \\ & A_2 & & & B_2 \\ & & \ddots & & \vdots \\ & & & A_i & B_i \end{bmatrix} \begin{bmatrix} u_1 \\ u_2 \\ \vdots \\ u_i \\ v \end{bmatrix} = \begin{bmatrix} b_1 \\ b_2 \\ \vdots \\ b_i \end{bmatrix} \tag{2}$$

As specified in Sect. 6.3 of Björck 1996 (see also Golub and van Loan 1989, Bierman 1977), the angular block structure of matrix $[A\ B]$ is well suited to recursive QR factorization. When dealing with large-scale problems, numerical accuracy can thereby be improved.

More interestingly, the corresponding techniques prove to be very efficient for GNSS data processing and quality control; see, e.g., Tiberius (1998), Loehnert *et al* (2000), Chang and Guo (2005). As clarified in this paper, this is particularly the case for the GNSS centralized approaches, even when dealing with small-scale systems. In particular, in the quality-control procedures, the identification of biases is then made easier (see Sects. 4.3 and 3.3).

To introduce the reader to the QR implementation of these approaches, we now concentrate on the simple case of continuous observations in RTK mode with a local-scale single baseline (see, e.g., Table 1 in Feng and Li 2008). This problem can of course be dealt with as a special case of multiple-baseline networks with possibly missing data. In this paper, we will not proceed that way. Indeed, the corresponding theoretical framework would then mask the main guidelines of our contribution.

The RD approach presented in Lannes 2007ab addressed this particular GNSS system. The corresponding data-assimilation procedure was based on recursive least-square (RLS) filtering. In particular, the normal equation associated with Eq. (2) was solved with the aid of classical RLS techniques. The QR implementation of this procedure therefore remained to be done.

As revealed by the contents of the present paper, this implementation led us to clarify some important points. For example, the RD concept was revisited and generalized. The quality-control procedure was thereby strongly simplified. At last but not the least, the advantages of the RD and DD approaches were conjugated in a straightforward manner. As a result, the extension to general networks presented in Lannes 2008 is to be revisited accordingly. This will be done in a forthcoming paper.

1.1 Observational equations

The particular GNSS system examined in this paper is governed by the following observational equations (see, e.g., Sect. 14 in Strang and Borre 1997). For each frequency f_ν, for each receiver-satellite pair (r, s), and at each epoch t, the carrier-phase and code relations are respectively of the form

$$\begin{aligned}\phi_{\nu,t}(r,s) = \rho_t(r,s) + c[\delta t_{\nu,t}(r) - \delta t_{\nu,t}(s)] \\ + \lambda_\nu[\varphi_{\nu,0}(r) - \varphi_{\nu,0}(s)] + \lambda_\nu N_\nu(r,s) + \varepsilon_{\nu,t}(r,s)\end{aligned} \tag{3}$$

$$p_{\nu,t}(r,s) = \rho_t(r,s) + c[\mathrm{d}t_{\nu,t}(r) - \mathrm{d}t_{\nu,t}(s)] + \epsilon_{\nu,t}(r,s) \tag{4}$$

In these equations, which are expressed in length units, $\rho_t(r,s)$ is the receiver-satellite range: the distance between satellite s (at the time $t-\tau$ where the signal is emitted) and receiver r (at the time t of its reception). The λ_ν's denote the wavelengths of the carrier waves; the integers $N_\nu(r,s)$ are the integer carrier-phase ambiguities. The instrumental delays and clock errors that for a given (ν,t) depend only on r and s are lumped together in the receiver and satellite error terms $\delta t_{\nu,t}(r)$, $\delta t_{\nu,t}(s)$ for the phase, and $\mathrm{d}t_{\nu,t}(r)$, $\mathrm{d}t_{\nu,t}(s)$ for the code (c is the speed of light); $\varphi_{\nu,0}(r)$ and $\varphi_{\nu,0}(s)$ are the initial phases (expressed in cycles) in receiver r and satellite s, respectively. The phase and code errors $\varepsilon_{\nu,t}(r,s)$ and $\epsilon_{\nu,t}(r,s)$ include both noise and residual model errors. Here, for clarity, the ionospheric and tropospheric delays are ignored (see Sect. 1.2 with a local-scale system).

For clarity, we now restrict ourselves to the single-frequency case. Equations (3) and (4) then reduce to

$$\begin{aligned}\phi_t(r,s) = \rho_t(r,s) + c[\delta t_t(r) - \delta t_t(s)] \\ + \lambda[\varphi_0(r) - \varphi_0(s)] + \lambda N(r,s) + \varepsilon_t(r,s)\end{aligned} \tag{5}$$

$$p_t(r,s) = \rho_t(r,s) + c[\mathrm{d}t_t(r) - \mathrm{d}t_t(s)] + \epsilon_t(r,s) \tag{6}$$

It may be convenient to consider that a function $\vartheta(r,s)$, such as $\rho_t(r,s)$ for example, takes its values on a rectangular grid. When the system includes two receivers and n satellites (as it is the case here), this grid includes two lines and n columns; the values $\vartheta(r,s)$ then define a vector $\boldsymbol{\vartheta}$ of the 'observational space' $\mathbb{R}^{2n}$. These values are the components of $\boldsymbol{\vartheta}$ in the standard basis of $\mathbb{R}^{2n}$.

The variance-covariance matrix of the data vector $\boldsymbol{\psi} = \boldsymbol{\phi}$ (for the phase) or $\boldsymbol{\psi} = \boldsymbol{p}$ (for the code) is denoted by $V_{\boldsymbol{\psi}}$. Let $[\boldsymbol{\vartheta}]$ now be the column matrix whose entries are the components of $\boldsymbol{\vartheta}$. The size $\|\boldsymbol{\vartheta}\|_{\boldsymbol{\psi}}$ of a vector $\boldsymbol{\vartheta}$ of type $\boldsymbol{\psi}$ (for example, that of an observational residual of type $\boldsymbol{\psi}$) is defined via the relation

$$\|\boldsymbol{\vartheta}\|^2_{\boldsymbol{\psi}} := [\boldsymbol{\vartheta}]^{\mathrm{T}} V_{\boldsymbol{\psi}}^{-1} [\boldsymbol{\vartheta}] \tag{7}$$

1.2 SD equations

Let r_1 be the reference receiver, and r_2 be that of the user. Denote by $s_1, s_2, \ldots, s_n$ the satellites involved in the GNSS device at epoch t. A quantity such as

$$\vartheta^{(j)} := \vartheta(r_2\,, s_j) - \vartheta(r_1\,, s_j) \tag{8}$$

is then referred to as a single difference (SD) in ϑ. (In this paper, a notation such as $a := b$ means 'a is equal to b by definition.')

Adopting the notation defined in Eq. (8), we then obtain from Eq. (5) the SD phase equations

$$\phi_t^{(j)} = \rho_t^{(j)} + \lambda v^{(j)} + \alpha_t + \varepsilon_t^{(j)} \qquad (j = 1, \ldots, n) \tag{9}$$

where

$$v^{(j)} := N^{(j)} - N^{(1)} \tag{10}$$

and

$$\begin{aligned} \alpha_t := c[\delta t_t(r_2) - \delta t_t(r_1)] \\ + \lambda[\varphi_0(r_2) - \varphi_0(r_1)] + \lambda N^{(1)} \end{aligned} \tag{11}$$

According to its definition, α_t is an unknown receiver parameter shifted by an unknown number of wavelengths. The $n-1$ integers

$$v^{(2)}, v^{(3)}, \ldots, v^{(n)}$$

are the DD ambiguities of the problem; here, the latter are defined with regard to the first satellite of the list of visible satellites at the initialization epoch: $v^{(1)} = 0$. This pointed out, in the present approach, no 'usual double difference' is computed: the SD data are dealt with in a homogeneous manner (see Sect. 1.4).

The SD code equations are obtained from Eq. (6) in a similar manner:

$$p_t^{(j)} = \rho_t^{(j)} + a_t + \epsilon_t^{(j)} \qquad (j = 1, \ldots, n) \tag{12}$$

where

$$a_t := c[\mathrm{d}t_t(r_2) - \mathrm{d}t_t(r_1)] \tag{13}$$

1.3 Linearized SD equations

The position variable at epoch t, ξ_t, appears via the linearization of the single differences $\rho_t^{(j)}$ with respect to the position variable $\xi_{2;t}$ of the user receiver r_2. Here, we implicitly refer to the relation $\xi_{2;t} = \tilde{\xi}_{2;t} + \xi_t$. As

$$\rho_t^{(j)} = \rho_t(r_2, s_j) - \rho_t(r_1, s_j)$$

the linear expansion of $\rho_t^{(j)}$ is of the form

$$\rho_t^{(j)} = \tilde{\rho}_t^{(j)} + \left(\kappa_t^{(j)} \cdot \xi_t\right) \tag{14}$$

where $\kappa_t^{(j)}$ is the unitary vector that characterizes the direction $s_j \to r_2$ of the signal received at epoch t. The geometry-free SD equations (9) and (12) then yield the linearized SD equations

$$\left(\kappa_t^{(j)} \cdot \xi_t\right) + \lambda v^{(j)} + \alpha_t + \varepsilon_t^{(j)} = \tilde{\phi}_t^{(j)} \tag{15}$$

$$\left(\kappa_t^{(j)} \cdot \xi_t\right) + a_t + \epsilon_t^{(j)} = \tilde{p}_t^{(j)} \tag{16}$$

where (for $j = 1, \ldots, n$)

$$\tilde{\phi}_t^{(j)} := \phi_t^{(j)} - \tilde{\rho}_t^{(j)} \tag{17}$$

$$\tilde{p}_t^{(j)} := p_t^{(j)} - \tilde{\rho}_t^{(j)} \tag{18}$$

We now show how to express these equations in a more concise form. Denoting by $\{e_j\}_{j=1}^n$ the standard basis of $\mathbb{R}^n$, let us consider the vector

$$\vartheta := \sum_{j=1}^{n} \vartheta^{(j)} e_j \tag{19}$$

where the $\vartheta^{(j)}$'s are the SD's defined in Eq. (8); $\mathbb{R}^n$ is then regarded as the 'SD space.' Throughout this paper, to avoid any confusion, a function such as $\vartheta(r, s)$ is never denoted by the isolated symbol ϑ.

Let Γ_t be the operator defined by the relations

$$(\Gamma_t \xi_t)^{(j)} := \left(\kappa_t^{(j)} \cdot \xi_t\right) \qquad (j = 1, \ldots, n) \tag{20}$$

By construction, the elements of the j^{th} line of the matrix of Γ_t are the components of $\kappa_t^{(j)}$, i.e., the direction cosines of $\kappa_t^{(j)}$; this matrix includes n lines. Let us now denote by ζ be the vector of $\mathbb{R}^n$ whose components are all equal to unity. In terms of vectors, the linearized SD equations (15) and (16) can then be written as follows:

$$\Gamma_t \xi_t + \lambda v + \zeta \alpha_t + \varepsilon_t = \tilde{\phi}_t \tag{21}$$

$$\Gamma_t \xi_t + \zeta a_t + \epsilon_t = \tilde{p}_t \tag{22}$$

Note that ξ_t, α_t and a_t are local variables, whereas v is a global variable.

Let $[\vartheta]$ now be the column matrix whose entries are the components of ϑ. The size $\|\vartheta\|_\psi$ of a vector ϑ of type ψ (for example, that of an observational residual of type ψ) is defined via the relation

$$\|\vartheta\|_\psi^2 := [\vartheta]^{\mathrm{T}} V_\psi^{-1} [\vartheta] \tag{23}$$

where V_ψ is variance-covariance matrix of ψ:

$$V_\psi = \mathcal{S} V_{\boldsymbol{\psi}} \mathcal{S}^{\mathrm{T}} \tag{24}$$

Here, $\mathcal{S}$ is the matrix of the SD operator (see Eq. (8))

$$\mathcal{S}[\boldsymbol{\vartheta}] := [\vartheta] \tag{25}$$

Let us now introduce the Cholesky factorization

$$V_\psi^{-1} = U_\psi^{\mathrm{T}} U_\psi \tag{26}$$

where U_ψ is an invertible upper-triangular matrix. From Eq. (23), we then have

$$\|\vartheta\|_\psi^2 = [\vartheta]^{\mathrm{T}} U_\psi^{\mathrm{T}} U_\psi [\vartheta] = [U_\psi \vartheta]^{\mathrm{T}} [U_\psi \vartheta]$$

i.e.,

$$\|\vartheta\|_\psi^2 = [\vartheta_\psi]^{\mathrm{T}} [\vartheta_\psi] \tag{27}$$

where

$$[\vartheta_\psi] := U_\psi [\vartheta] \tag{28}$$

According to these equations, the size of a vector ϑ of type ψ is equal to the size of ϑ_ψ in $\mathbb{R}^n$:

$$\|\vartheta\|_\psi^2 = \|\vartheta_\psi\|^2 \tag{29}$$

As clarified in Sect. 1.4, this trick proves to play a key role in the approach presented in this paper.

1.4 Statement of the problem

Let t_1 be the initialization epoch of the 'current run' $[t_1, \ldots, t_i]$. According to Eqs. (21) and (22), the problem is to minimize the objective functional

$$\begin{aligned} f(\xi_1, \ldots, \xi_i; v; \alpha_1, \ldots, \alpha_i; a_1, \ldots, a_i) \\ := \sum_{\iota=1}^{i} \|\tilde{\phi}_\iota - (\Gamma_\iota \xi_\iota + \lambda v) - \zeta \alpha_\iota\|_{\phi_\iota}^2 \\ + \|\tilde{p}_\iota - \Gamma_\iota \xi_\iota - \zeta a_\iota\|_{p_\iota}^2 \end{aligned} \tag{30}$$

where $\xi_\iota \equiv \xi_{t_\iota}$, and likewise for α_ι, a_ι, $\tilde{\phi}_\iota$, $\tilde{p}_\iota$ and Γ_ι. In our approach, this is done in two steps. The first step is to minimize f in α_ι and a_ι for $\iota = 1, \ldots, i$. As clarified below, this operation corresponds to the notion of 'reduction.'

1.4.1 Reduced equations

Let us first concentrate on the phase terms. For clarity, let us then set $\vartheta := \tilde{\phi}_\iota - (\Gamma_\iota \xi_\iota + \lambda v)$. The optimal estimate of α_ι is then the real number $\alpha_\circ$ for which the minimum of $\|\vartheta - \zeta\alpha\|_\phi$ in α is attained. From Eq. (29), we have

$$\|\vartheta - \zeta\alpha\|_\phi^2 = \|\vartheta_\phi - \zeta_\phi \alpha\|^2$$

where ϕ stands for ϕ_ι. As a result, $\alpha_\circ$ is the solution of the normal equation

$$[\zeta_\phi]^{\mathrm{T}}[\zeta_\phi]\alpha = [\zeta_\phi]^{\mathrm{T}}[\vartheta_\phi]$$

i.e.,

$$\alpha_\circ = \frac{[\zeta_\phi]^{\mathrm{T}}[\vartheta_\phi]}{[\zeta_\phi]^{\mathrm{T}}[\zeta_\phi]}$$

It follows that

$$\vartheta_\phi - \zeta_\phi \alpha_\circ = \mathcal{R}_\phi \vartheta$$

where (here, for $\psi = \phi \equiv \phi_\iota$)

$$\mathcal{R}_\psi \vartheta := \vartheta_\psi - \frac{[\zeta_\psi]^{\mathrm{T}}[\vartheta_\psi]}{[\zeta_\psi]^{\mathrm{T}}[\zeta_\psi]}\,\zeta_\psi \tag{31}$$

Consequently (see Eq. (30)):

$$\min_{\alpha_\iota \in \mathbb{R}} \|\tilde{\phi}_\iota - (\Gamma_\iota \xi_\iota + \lambda v) - \zeta\alpha_\iota\|_{\phi_\iota}^2 = \|\mathcal{R}_{\phi_\iota}[\tilde{\phi}_\iota - (\Gamma_\iota \xi_\iota + \lambda v)]\|^2$$

Likewise, for the code terms,

$$\min_{a_\iota \in \mathbb{R}} \|\tilde{p}_\iota - \Gamma_\iota \xi_\iota - \zeta a_\iota\|_{p_\iota}^2 = \|\mathcal{R}_{p_\iota}(\tilde{p}_\iota - \Gamma_\iota \xi_\iota)\|^2$$

We are thus led to minimize the 'reduced functional'

$$\begin{aligned} f_{\mathrm{r}}(\xi_1, \ldots, \xi_i; v) \\ := \sum_{\iota=1}^{i} \|\mathcal{R}_{\phi_\iota}[\tilde{\phi}_\iota - (\Gamma_\iota \xi_\iota + \lambda v)]\|^2 \\ + \|\mathcal{R}_{p_\iota}(\Gamma_\iota \xi_\iota - \tilde{p}_\iota)\|^2 \end{aligned} \tag{32}$$

The 'reduced equations' to be solved in the usual LS sense can therefore be displayed as follows:

$$\mathcal{R}_{\phi_\iota}(\Gamma_\iota \xi_\iota + \lambda v) = \mathcal{R}_{\phi_\iota}\tilde{\phi}_\iota \tag{33}$$

$$\mathcal{R}_{p_\iota}\Gamma_\iota \xi_\iota = \mathcal{R}_{p_\iota}\tilde{p}_\iota \tag{34}$$

1.4.2 Reduction operator

Let us concentrate on the 'reduction operator' (31). For clarity, let us set

$$\vartheta_{\mathrm{r};\psi} := \mathcal{R}_\psi \vartheta \tag{35}$$

To give a more concrete idea of the action of this operator, let us now consider the typical situation where the variance-covariance matrix of the observational data of type $\boldsymbol{\psi}$ is of the form (see Liu 2002)

$$V_{\boldsymbol{\psi}} = \mathrm{diag}\big(\eta(r,s)\,\sigma_{\boldsymbol{\psi}}^2\big) \tag{36}$$

Here, $\sigma_{\boldsymbol{\psi}}^2$ is a 'reference variance;' $\eta(r,s)$ is a nonnegative weight function. The variance-covariance matrix of the SD data is then given by the relation (see Eq. (24))

$$V_\psi = \mathrm{diag}(\eta_j \sigma_{\boldsymbol{\psi}}^2) \qquad \eta_j := \eta(r_1\,, s_j) + \eta(r_2\,, s_j) \tag{37}$$

From Eq. (26), we then have

$$U_\psi = \mathrm{diag}\left(\frac{1}{\sqrt{\eta_j}\,\sigma_{\boldsymbol{\psi}}}\right) \tag{38}$$

hence, from Eq. (28),

$$\vartheta_\psi^{(j)} = \frac{1}{\sqrt{\eta_j}\,\sigma_{\boldsymbol{\psi}}}\,\vartheta^{(j)} \qquad \zeta_\psi^{(j)} = \frac{1}{\sqrt{\eta_j}\,\sigma_{\boldsymbol{\psi}}}\,\zeta^{(j)}$$

As $\zeta^{(j)} = 1$ for all j, we then have

$$[\zeta_\psi]^{\mathrm{T}}[\vartheta_\psi] = \frac{1}{\sigma_{\boldsymbol{\psi}}^2}\sum_{j=1}^{n}\frac{1}{\eta_j}\vartheta^{(j)} \qquad [\zeta_\psi]^{\mathrm{T}}[\zeta_\psi] = \frac{1}{\sigma_{\boldsymbol{\psi}}^2}\sum_{j=1}^{n}\frac{1}{\eta_j}$$

It then follows from Eqs. (35) and (31) that the components of $\vartheta_{\mathrm{r};\psi}$ are given by the formula

$$\vartheta_{\mathrm{r};\psi}^{(j)} = \frac{\vartheta^{(j)} - \vartheta^{(0)}}{\sigma_{\psi j}} \qquad \sigma_{\psi j} := \sqrt{\eta_j}\,\sigma_{\boldsymbol{\psi}} \tag{39}$$

where

$$\vartheta^{(0)} := \sum_{j=1}^{n} \mu_j \vartheta^{(j)} \qquad \mu_j := \frac{\frac{1}{\eta_j}}{\sum_{k=1}^{n}\frac{1}{\eta_k}} \tag{40}$$

Note that $\sigma_{\psi j}$ is the standard deviation of the single-difference $\psi^{(j)}$. With regard to the SD weights $1/\eta_j$ or $1/\sigma_{\psi j}^2$, $\vartheta^{(0)}$ is a 'barycentric single difference:'

$$\sum_{j=1}^{n}\frac{\vartheta^{(j)} - \vartheta^{(0)}}{\sigma_{\psi j}^2} = 0$$

According to its notation, this virtual single difference is associated with a virtual satellite s_0. The n 'virtual double differences' $\vartheta^{(j)} - \vartheta^{(0)}$ can thus be regarded as the 'centralized values' of the $\vartheta^{(j)}$'s (Shi and Han 1992), or equally well, as the 'reduced values' of the $\vartheta^{(j)}$'s (Lannes 2007ab). Indeed, the minimum of

$$\sum_{j=1}^{n}\frac{(\vartheta^{(j)} - \omega)^2}{\sigma_{\psi j}^2} \qquad (\omega \in \mathbb{R})$$

is obtained for $\omega = \vartheta^{(0)}$. In other terms, in a concrete manner, the action of $\mathcal{R}_\psi$ consists in performing this type of reduction.

1.5 Contents

As specified in Sect. 2, the reduced equations (33) and (34) lead to a linear system of type (2). The block matrices A_i, B_i and b_i are then defined, and likewise for the local variables $u_1, u_2, \ldots, u_i$ and the global variable v. The components of v are then the float ambiguities of the problem.

The float solution $\hat{v}$ is refined recursively, epoch-by-epoch, with the aid of the QR method. This method is introduced in Sect. 3.1, and fully described in Sect. 3.2. The selected QR implementation is based on 'Givens rotations' (see, e.g., Björck 1996); the corresponding operations can thus be stored in memory very easily. This is very useful for the variational method presented in Sect. 3.3. As the latter is basically involved in the quality-control procedures (see Sect. 4), the efficiency of the DIA method presented in Lannes 2007b is thereby improved. The state transitions induced by the appearance and/or the disappearance of some satellites are examined in Sects. 3.4 and 3.5, respectively. As specified in Sect. 3.6, the inverse of the variance-covariance matrix of $\hat{v}$ is directly provided by the QR method. The procedure that yields the integer-ambiguity solution $\check{v}$ is described in that section.

This study is illustrated with dual-frequency examples (Sect. 5). Some comments on the key points of our contribution, and its extension to GNSS networks are to be found in Sect. 6.

2 Block matrices of the global RD equation

The reduced equations (33) and (34) lead to an equation of type (2). We now clarify this point explicitly. The extension to the dual-frequency case is straightforward (see Sect. 5).

The local variable u_i then reduces to the position variable ξ_i. The block matrix A_i is then defined as follows:

$$A_i = \begin{bmatrix} \mathcal{R}_{\phi_i} \Gamma_i \\ \mathcal{R}_{p_i} \Gamma_i \end{bmatrix} \tag{41}$$

Note that $\mathcal{R}_\psi \Gamma_i$ is obtained by applying the reduction operator $\mathcal{R}_\psi$ to each column vector of Γ_i (see Eq. (31) and Sect. 1.4.2). The corresponding data block of Eq. (2) is then

$$b_i = \begin{bmatrix} \mathcal{R}_{\phi_i} \tilde{\phi}_i \\ \mathcal{R}_{p_i} \tilde{p}_i \end{bmatrix} \tag{42}$$

Let $\bar{\mathrm{S}}_i := \{s_1, s_2, \ldots, s_{\bar{n}_i}\}$ be the series of satellites involved in the observational process until epoch t_i included. A given satellite may disappear and reappear in the same run. Such a satellite is then regarded as a new satellite. In other words, whenever this occurs, a new satellite is added at the end of this series. The n_i satellites of epoch t_i form a subset S_i of $\bar{\mathrm{S}}_i$: $n_i \leq \bar{n}_i$.

To introduce the reader to what is essential, we first restrict ourselves to the case where no satellite appears or disappears in the current run $[t_1, \ldots, t_i]$: no state transition in this interval. The entries of the global variable v are then the ambiguities $v^{(2)}$, $v^{(3)}, \ldots, v^{(n_i)}$ with $n_i = \bar{n}_i$ (see Eq. (10)). As clarified in Sect. 3.4, it is recommended to class these ambiguities in reverse order. For example, for $n_i = 7$, the global variable v is then explicitly defined as the column matrix (with 6 entries)

$$v = \begin{bmatrix} v^{(7)} \\ v^{(6)} \\ \vdots \\ v^{(3)} \\ v^{(2)} \end{bmatrix} \tag{43}$$

The phase block of B_i is then of the form (see Eq. (33)):

$$\left[B_i\right]_{\phi_i} = \mathcal{R}_{\phi_i}^{[n_i]} \begin{bmatrix} \cdot & \cdot & \cdot & \cdot & \cdot & \cdot \\ \cdot & \cdot & \cdot & \cdot & \cdot & \lambda \\ \cdot & \cdot & \cdot & \cdot & \lambda & \cdot \\ \cdot & \cdot & \cdot & \lambda & \cdot & \cdot \\ \cdot & \cdot & \lambda & \cdot & \cdot & \cdot \\ \cdot & \lambda & \cdot & \cdot & \cdot & \cdot \\ \lambda & \cdot & \cdot & \cdot & \cdot & \cdot \end{bmatrix} \quad (n_i = 7) \tag{44}$$

Here, the dots stand for 0. This matrix includes n_i lines (corresponding to the n_i visible satellites of the system), and $n_i - 1$ columns (corresponding to the $n_i - 1$ ambiguities of the problem). The notation $\mathcal{R}_{\phi_i}^{[n_i]}$ means that the reduction operation is performed on vectors of $\mathbb{R}^{n_i}$. Here, as the reference satellite s_1 of the current run is visible, the first line is nought (see Eqs. (9) and (10)).

Note that the code block of B_i is nought: $\left[B_i\right]_{p_i} = 0$.

3 QR method

We first introduce the reader to the notion of QR factorization (Sect. 3.1). We then show how to solve Eq. (2) in a recursive manner (Sect. 3.2). The corresponding variational aspects are presented in Sect. 3.3. We then specify how to handle the ambiguities when some satellites appear and/or disappear (Sects. 3.4 and 3.5, respectively). Finally, Sect. 3.6 is devoted to the QR aspects concerning the integer ambiguity problem.

3.1 QR factorization

Let us consider the following general LS problem: minimize, with the Euclidean norm,

$$\|\mathrm{A}x - y\|^2_{\mathbb{R}^{\mathrm{m}}} \quad (\mathrm{A} \in \mathbb{R}^{\mathrm{m}\times\mathrm{n}},\ \mathrm{m} \geq \mathrm{n},\ \mathrm{rank\ A} = \mathrm{n})$$

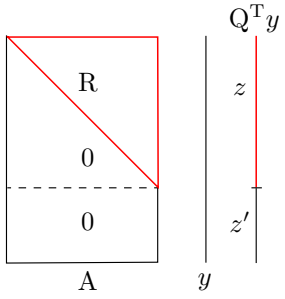

Fig. 1 *LS solution via QR factorization.* The action of Q^{T} on A and y yields the basic QR structure sketched here: the upper-triangular matrix R and the column matrix z. The solution of the equation $\mathrm{A}x = y$ in the LS sense is then given by the formula $x = \mathrm{R}^{-1}z$ (see Eq. (46)).

With regard to numerical accuracy, the best way to solve this problem is to use a method based on the QR factorization of A (see, e.g., Björck 1996):

$$\mathrm{A} = \mathrm{Q}\begin{bmatrix} \mathrm{R} \\ 0 \end{bmatrix} \tag{45}$$

where $\mathrm{R} \in \mathbb{R}^{\mathrm{n}\times\mathrm{n}}$ is an upper triangular matrix with positive diagonal terms, and $\mathrm{Q} \in \mathbb{R}^{\mathrm{m}\times\mathrm{m}}$ is an orthogonal matrix: $\mathrm{Q}^{\mathrm{T}}\mathrm{Q} = \mathrm{I_m}$ (the identity matrix on $\mathbb{R}^{\mathrm{m}}$). We thus have

$$\begin{aligned} \|\mathrm{A}x - y\|^2_{\mathbb{R}^{\mathrm{m}}} &= \|\mathrm{Q}^{\mathrm{T}}(\mathrm{A}x - y)\|^2_{\mathbb{R}^{\mathrm{m}}} \\ &= \left\|\mathrm{Q}^{\mathrm{T}}\mathrm{Q}\begin{bmatrix} \mathrm{R} \\ 0 \end{bmatrix} x - \mathrm{Q}^{\mathrm{T}}y\right\|^2_{\mathbb{R}^{\mathrm{m}}} \end{aligned}$$

Setting $\mathrm{Q}^{\mathrm{T}}y = z + z'$ where $z \in \mathbb{R}^{\mathrm{n}}$ (see Fig. 1), it follows that

$$\|\mathrm{A}x - y\|^2_{\mathbb{R}^{\mathrm{m}}} = \|\mathrm{R}x - z\|^2_{\mathbb{R}^{\mathrm{n}}} + \|z'\|^2_{\mathbb{R}^{\mathrm{m}-\mathrm{n}}} \tag{46}$$

The LS solution is therefore given by the relation

$$\hat{x} = \mathrm{R}^{-1}z \tag{47}$$

The problem can thereby be solved by back substitution. In the case where x is confined to $\mathbb{Z}^{\mathrm{n}}$, the solution of the problem is therefore defined as follows:

$$\dot{x} = \underset{x\in\mathbb{Z}^{\mathrm{n}}}{\operatorname{argmin}} \|\mathrm{R}(x - \hat{x})\|^2_{\mathbb{R}^{\mathrm{n}}} \tag{48}$$

Indeed, $\mathrm{R}x - z = \mathrm{R}(x - \hat{x})$.

According to Eq. (45), QR factorization consists in finding an operator Q^{T} (and thereby an operator Q) such that $\mathrm{Q}^{\mathrm{T}}\mathrm{A}$ has the block structure $[\mathrm{R}\ 0]^{\mathrm{T}}$ sketched in Fig. 1. This operator is defined as a product of elementary orthogonal transformations. In the implementation presented in this paper, the latter are Givens rotations (see Eqs. (2.3.10) to (2.3.13) in Björck 1996). Premultiplication of A and y by such a rotation matrix affects only rows k and ℓ of A and d. This matrix is defined so that, for $(\mathrm{a}_k^2 + \mathrm{a}_\ell^2) \neq 0$,

$$\begin{bmatrix} \mathrm{c} & \mathrm{s} \\ -\mathrm{s} & \mathrm{c} \end{bmatrix}\begin{bmatrix} \mathrm{a}_k \\ \mathrm{a}_\ell \end{bmatrix} = \begin{bmatrix} \mathrm{a} \\ 0 \end{bmatrix} \tag{49}$$

where

$$\mathrm{a} = (\mathrm{a}_k^2 + \mathrm{a}_\ell^2)^{1/2} \tag{50}$$

It is easy to check that the cosine and sinus values c and s are then given by the following formulas

$$\mathrm{c} = \mathrm{a}_k/\mathrm{a} \qquad \mathrm{s} = \mathrm{a}_\ell/\mathrm{a} \tag{51}$$

Note that $\mathrm{m}-1$ Givens rotations are required for the first column of A, $\mathrm{m}-2$ for the second, and so on (see Fig. 1). It is important to point out that that the action of Q^{T} can be stored in memory as the sequence of the successive (cosine, sinus) pairs (c, s) characterizing the successive Givens rotations involved in this operation.

3.2 Recursive QR factorization

We now show how to solve, in the LS sense and recursively, the equation (2) induced by the reduced equations (33) and (34).

Let us first consider the initialization epoch: epoch 1. The problem is then solved in two steps (see Fig. 2). The Givens rotations of the first step are those required for finding the upper triangular matrix K_1. The modified version of B_1 thus obtained includes an upper block L_1 and a lower block L'_1. Likewise, the modified version of b_1 includes two column submatrices: c_1 and c'_1. The Givens rotations of the second step yield the upper triangular matrix R_1; c'_1 then yields $(d_1\,, d'_1)$; see Fig. 2. Note that K_1, L_1 and c_1 are not affected by these rotations. The global solution is then obtained by back substitution via the formula $\hat{v} = R_1^{-1}d_1$. The local solution can then be also computed by back substitution: $\hat{u}_1 = K_1^{-1}(c_1 - L_1\hat{v})$.

The first step of the next epoch (epoch 2) is similar to that of epoch 1: one thus obtains the upper triangular matrix K_2. The modified version of B_2 then includes an upper block L_2 and a lower block L'_2. Likewise, the modified version of b_2 includes two column submatrices: c_2 and c'_2 (see Fig. 2). The Givens rotations of the second step then operate on $(R_1\,, L'_2)$ and $(d_1\,, c'_2)$ so as to transform L'_2 into a zero block matrix. One thus gets R_2 and $(d_2\,, d'_2)$; $\hat{v}$ is then updated via the relation $\hat{v} = R_2^{-1}d_2$. The local solution at epoch 2 can then be computed: $\hat{u}_2 = K_2^{-1}(c_2 - L_2\hat{v})$.

In summary, one thus operates, recursively, with the key structure shown in Fig. 3: K_i, $(L_i\,, L'_i)$ and $(c_i\,, c'_i)$ are computed from A_i, B_i and b_i, R_i and $(d_i\,, d'_i)$ being then computed from $(R_{i-1}\,, L'_i)$ and $(d_{i-1}\,, c'_i)$. We then have

$$\begin{bmatrix} K_i & L_i \\ \cdot & R_i \end{bmatrix}\begin{bmatrix} \hat{u}_i \\ \hat{v} \end{bmatrix} = \begin{bmatrix} c_i \\ d_i \end{bmatrix} \tag{52}$$

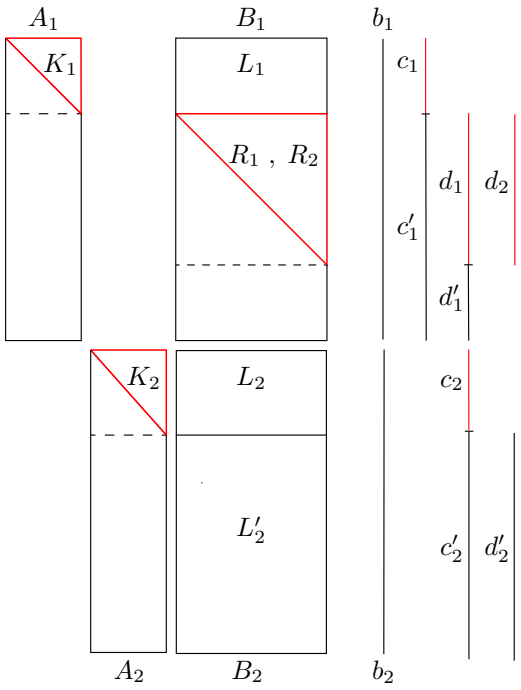

Fig. 2 *LS solution via recursive QR factorization.* The principle of the recursive QR method is sketched here for the first two epochs: epoch 1 with the input block matrices A_1 , B_1 and the data column matrix b_1; epoch 2 with the input block matrices A_2 , B_2 and the data column matrix b_2. The initialization process is performed in two steps: K_1 , $(L_1\,, L'_1)$, $(c_1\,, c'_1)$ are built in the first step (see text for L'_1), whereas R_1 , $(d_1\,, d'_1)$ are built in the second. The global float solution is then found by back substitution: $\hat{v} = R_1^{-1} d_1$. The local solution is then given by the formula $\hat{u}_1 = K_1^{-1}(c_1 - L_1\hat{v})$. Likewise, at the next epoch, one first builds K_2 , $(L_2\,, L'_2)$, $(c_2\,, c'_2)$, and then R_2, $(d_2\,, d'_2)$; $\hat{v}$ is then updated via the relation $\hat{v} = R_2^{-1} d_2$. The local solution at epoch 2 can then be computed: $\hat{u}_2 = K_2^{-1}(c_2 - L_2\hat{v})$.

hence $\hat{v} = R_i^{-1} d_i$ and $\hat{u}_i = K_i^{-1}(c_i - L_i\hat{v})$. The detailed implementation of this process must of course take account of the fact the code block of B_i is nought.

3.3 Variational calculation

We now answer to the following question: what are the variations $\Delta\hat{u}_i$ and $\Delta\hat{v}$ induced by a variation Δb_i of b_i (at epoch t_i)? From Eq. (2), these variations are the u-v components at epoch t_i of the LS solution of the equation

$$\begin{bmatrix} A_1 & & & B_1 \\ & A_2 & & B_2 \\ & & \ddots & \vdots \\ & & A_i & B_i \end{bmatrix} \begin{bmatrix} \Delta u_1 \\ \Delta u_2 \\ \vdots \\ \Delta u_i \\ \Delta v \end{bmatrix} = \begin{bmatrix} 0 \\ 0 \\ \vdots \\ \Delta b_i \end{bmatrix}$$

By construction, the quantities $\Delta d_1, \ldots, \Delta d_{i-1}$ induced by this equation are nought. The problem is therefore

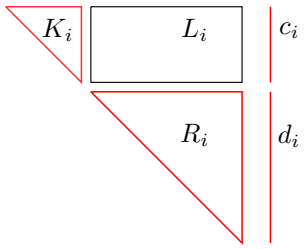

Fig. 3 *Recursive QR triangular structure.* According to the principle of the recursive QR method sketched in Fig. 2, the calculation of R_i and d_i requires to have kept in memory the upper triangular matrix R_{i-1} and the column matrix d_{i-1} (see text).

the same as previously, Δd_i being then computed from $\Delta c'_i$ with $\Delta d_{i-1} = 0$. This is why it is recommended to store in memory the sequence of the successive pairs (c, s) characterizing the Givens operators involved in the two QR steps of epoch t_i (see Fig. 2 and Eqs. (51) & (50)).

3.4 Handling the ambiguities when some satellites appear

As shown in Eq. (43), the ambiguities are put in reverse order. When some satellites appear at epoch t_i, the first columns of B_i can then be processed as the last columns of A_i (see Fig. 2). To get R_i and d_i, one then proceeds as illustrated in Fig. 4.

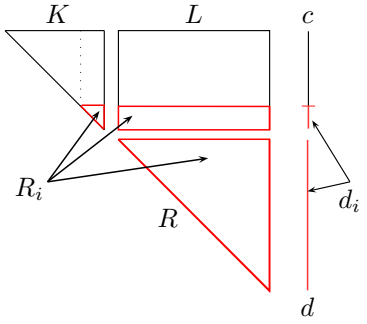

Fig. 4 *Handling additional ambiguities.* When satellites appear at epoch t_i, the first columns of B_i are processed as the last columns of A_i. The recursive QR operation then yields the quantities K, L, c, R and d. To get R_i and d_i, one then proceeds as illustrated here.

3.5 Handling the ambiguities when some satellites disappear

Let us first consider the case where the reference satellite of the current run disappears at epoch t_i. For example,

with regard to the situation corresponding to Eq. (44), the phase block of B_i then becomes

$$\left[B_i\right]_\phi = \mathcal{R}_\phi^{[n_i]} \begin{bmatrix} \cdot & \cdot & \cdot & \cdot & \cdot & \lambda \\ \cdot & \cdot & \cdot & \cdot & \lambda & \cdot \\ \cdot & \cdot & \cdot & \lambda & \cdot & \cdot \\ \cdot & \cdot & \lambda & \cdot & \cdot & \cdot \\ \cdot & \lambda & \cdot & \cdot & \cdot & \cdot \\ \lambda & \cdot & \cdot & \cdot & \cdot & \cdot \end{bmatrix} \qquad (n_i = 6) \quad (53)$$

The calculation of R_i and d_i is then performed as usually. Indeed, as the ambiguities to be considered remain the same, R_{i-1} and d_{i-1} must not be modified.

Let us now consider the case where, for example, the satellites s_7 and s_6 disappear at epoch t_i. The ambiguities v_7 and v_6 of Eq. (43) can then be removed. The phase block of B_i is then of the form (see Eq. (44))

$$\left[B_i\right]_\phi = \mathcal{R}_\phi^{[n_i]} \begin{bmatrix} \cdot & \cdot & \cdot & \cdot \\ \cdot & \cdot & \cdot & \lambda \\ \cdot & \cdot & \lambda & \cdot \\ \cdot & \lambda & \cdot & \cdot \\ \lambda & \cdot & \cdot & \cdot \end{bmatrix} \qquad (n_i = 5) \quad (54)$$

In the calculation of the upper triangular matrix R_i, R_{i-1} is then simply updated by removing its first two lines and first two columns. Likewise, in the calculation of d_i, the first two entries of d_{i-1} are then to be removed.

Let us now consider the case where, for example, satellites s_5 and s_3 disappear at epoch t_i, the phase block of B_i is then of the same as that defined in Eq. (54); R_{i-1} and d_{i-1} must then be modified as specified below.

One first performs the permutation

$$\begin{bmatrix} v^{(7)} \\ v^{(6)} \\ v^{(5)} \\ v^{(4)} \\ v^{(3)} \\ v^{(2)} \end{bmatrix} \longrightarrow \begin{bmatrix} v^{(5)} \\ v^{(3)} \\ v^{(7)} \\ v^{(6)} \\ v^{(4)} \\ v^{(2)} \end{bmatrix} \quad (55)$$

The columns of R_{i-1} are then permuted accordingly. As the matrix thus obtained, R'_{i-1}, is no longer upper triangular, one then performs Givens rotations on R'_{i-1} and d_{i-1} so that R'_{i-1} becomes upper triangular: $R'_{i-1} \to R''_{i-1}$, $d_{i-1} \to d''_{i-1}$. To complete the process, one then removes the first two lines and first two columns of R''_{i-1}, as well as the first two entries of d''_{i-1}.

3.6 Integer-ambiguity resolution

Let $\hat{v}$ be the float solution at epoch t_i, and $\mathfrak{n}$ be the number of its components. In single-frequency mode, depending on whether the reference satellite of the run $[t_1, t_i]$ is visible or not, $\mathfrak{n}$ is equal to $n_i - 1$ or n_i (respectively). The ambiguity solution is then defined by the relation (see Eq. (48))

$$\dot{v} = \underset{v \in \mathbb{Z}^{\mathfrak{n}}}{\operatorname{argmin}} \|R_i(v - \hat{v})\|^2_{\mathbb{R}^{\mathfrak{n}}} \quad (56)$$

According to this formula, $\dot{v}$ is the point of $\mathbb{Z}^{\mathfrak{n}}$ closest to $\hat{v}$, the distance being that induced by the quadratic form

$$q(v) := \|R_i v\|^2_{\mathbb{R}^{\mathfrak{n}}} = v^{\mathrm{T}}[R_i^{\mathrm{T}} R_i]v \quad (57)$$

Note that $R_i^{\mathrm{T}} R_i$ is the inverse of the variance-covariance matrix of $\hat{v}$:

$$R_i^{\mathrm{T}} R_i = V_{\hat{v}}^{-1} \quad (58)$$

The QR method thus provides the Cholesky factor R_i of the matrix of q directly. This is not the case in the usual RLS filtering techniques. Indeed, the latter provide $V_{\hat{v}}$ which is then to be inverted.

The nearest-lattice-point problem (56) is solved in two steps (see, e.g., Agrell et al. 2002). One first searches a 'reduced basis' of $\mathbb{Z}^{\mathfrak{n}}$ in which the matrix of q is as diagonal as possible. The problem is then solved in this basis by using the corresponding 'reduced form' of R_i: $\bar{R}_i$; the integer-valued solution $\dot{v}$ is then expressed in the original basis.

The first step corresponds to a decorrelation process. The decorrelation methods to be implemented must somehow refer to the principles of the LLL algorithm (an algorithm devised by Lenstra, Lenstra and Lovàsz in 1982). Here, as the QR recursive process provides R_i directly, the LLL implementations of Luk and Tracy (2008) are well suited to the problem. Denoting by $\bar{r}_{k,\ell}$'s the matrix elements of $\bar{R}_i$, the following conditions can thus be imposed:

(i) $\bar{r}_{k,k} > 2|\bar{r}_{k,\ell}|$ (for $1 \le k < \ell \le \mathfrak{n}$)

(ii) $\bar{r}^2_{k,k} \ge (\omega - 1/4)\bar{r}^2_{k-1,k-1}$ (for $2 \le k \le \mathfrak{n}$)

with $1/4 < \omega < 1$. In practice, to speed up the second-step procedure, ω is set equal to 0.999. Note that Condition (ii) is not necessarily imposed in other decorrelation methods (see, e.g., Xu 2001).

When in the data assimilation process, $\dot{v}$ becomes consistent with the model, the ambiguities are said to be fixed. The local variable $\hat{u}_i$ is then refined via a fixed least-squares (FLS) process, i.e., a process in which the ambiguities are fixed at these values. Again, the QR method is well suited to solving these problems.

4 Quality control

To prevent that biases on the SD data propagate undetected into the ambiguity solution and the positioning results, particular methods have been developed. The biases are first 'detected,' then 'identified,' and finally the results are 'adapted' consequently (e.g., Teunissen 1990, Hewitson et al. 2004). Note that these DIA methods are to be implemented in all the modes to be considered: LS, RLS and FLS.

The DIA method presented in this section is a simplified version of that presented in Lannes 2007b. Its identification principle is 'local,' in the sense that the biases thus

identified concern only the data of the current epoch. In the present version, the corresponding analysis is based on the results provided by the QR process at that epoch. When the ambiguities are not fixed, the adaptation principle is global: the local position, the current biases, the current float ambiguities and the current QR triangular structure (sketched in Fig. 3) are updated in the global frame of the QR recursive process, without any approximation. This was not completely the case in Lannes 2007b.

4.1 Local identification

The identification principle is based on the analysis of the residual at epoch t_i:

$$w_i := b_i - (A_i \hat{u}_i + B_i \hat{v}) \tag{59}$$

Note that $\hat{u}_i$ and $\hat{v}$ depend on b_i in a linear manner. Let us now denote by y_i the column matrix of the SD data corrected from the terms due to linearization (see Eqs. (42))

$$y_i := \begin{bmatrix} \tilde{\phi}_i \\ \tilde{p}_i \end{bmatrix} \tag{60}$$

In what follows, H_i is the operator that yields w_i from y_i (see Eqs. (42) and (59)):

$$w_i = H_i y_i \tag{61}$$

For clarity, we now omit subscript i. Denoting by w_p and w_ϕ the code and phase components of w (respectively), we then have, in single-frequency mode,

$$\|w\|^2 := \|w_\phi\|^2 + \|w_p\|^2 \tag{62}$$

where $\|w_\psi\|^2 = \sum_{j_\psi=1}^{n} |w_{j_\psi}|^2$ for $\psi = p$ or ϕ. When $\|w\|^2$ is too large (see Sect. 4.3), we then search to identify, in the SD data y, a global bias of the form

$$z = \begin{bmatrix} \sum_{j_\phi \in \Omega_\phi} \beta_{j_\phi} e_{j_\phi} \\ \sum_{j_p \in \Omega_p} \beta_{j_p} e_{j_p} \end{bmatrix} \tag{63}$$

The 'outlier sets' Ω_ϕ and Ω_p are some 'small subsets' of $\{1, \ldots, n\}$. With regard to the phase (for example) the corresponding SD model is the following (see Eq. (9)):

$$\rho^{(j)} + \lambda v^{(j)} + \alpha + \varepsilon^{(j)} = \begin{cases} \phi^{(j)} - \beta_{j_\phi} & \text{if } j \in \Omega_\phi \\ \phi^{(j)} & \text{otherwise} \end{cases}$$

The problem is to identify Ω_ϕ and Ω_p while getting least-squares estimates of the corresponding biases β_{j_ϕ} and β_{j_p}. The guiding idea is to the consider the contribution of these biases to w.

As $\Delta w = H\,\Delta y$ (see Eq. (61)), we must first see what is the contribution of these biases to y. At this level, the correction terms induced by e_{j_ϕ} and e_{j_p} are denoted by z_{j_ϕ} and z_{j_p}:

$$y \overset{\text{set}}{=} y - z_{j_\psi} \qquad z_{j_\phi} := \begin{bmatrix} e_{j_\phi} \\ 0 \end{bmatrix} \quad z_{j_p} := \begin{bmatrix} 0 \\ e_{j_p} \end{bmatrix} \tag{64}$$

A notation such as $a \overset{\text{set}}{=} a + b$ means 'a is set equal to the current value of $a+b$.' The variations of w induced by e_{j_ϕ} and e_{j_p} are therefore characterized by the quantities f_{j_ϕ} and f_{j_p} defined below:

$$w \overset{\text{set}}{=} w - H z_{j_\psi} \qquad f_{j_\phi} := H z_{j_\phi} \qquad f_{j_p} := H z_{j_p} \tag{65}$$

As a result, the variation of w induced by the global bias z is characterized by the vector

$$Mz := \sum_{j_\phi \in \Omega_\phi} \beta_{j_\phi} f_{j_\phi} + \sum_{j_p \in \Omega_p} \beta_{j_p} f_{j_p} \tag{66}$$

We are then led to solve, in the least-square sense, the equation $w - Mz \,`='\, 0$, in which the column vectors of M, the f_{j_ϕ}'s and f_{j_p}'s, have to be thoroughly selected. As clarified in Sect. 4.3, this operation is performed via a particular Gram-Schmidt orthogonalization process which is interrupted as soon as the corrected data are consistent with the model.

4.2 Global adaptation

Once the outlier sets Ω_ϕ and Ω_p have been identified, the model is to be updated consequently: A_i is completed by adding the columns associated with the corresponding bias variables β_{j_ϕ} and β_{j_p}. From Eqs. (42) and (64), these column matrices are respectively of the form

$$\begin{bmatrix} \mathcal{R}_\phi e_{j_\phi} \\ 0 \end{bmatrix} \qquad \begin{bmatrix} 0 \\ \mathcal{R}_p e_{j_p} \end{bmatrix} \tag{67}$$

The global QR recursive process is then updated accordingly. The position variable, the SD biases and the float ambiguities are thus refined, as well as R_i and d_i in particular (see Fig. 3). When the QR process is initialized, or when the ambiguities are fixed, the SD biases provided by the adaptation process coincide with those provided by the identification procedure (see Sect. 4.1 and steps *2.4* & *2.5* in Sect. 4.3). The LS problem to be solved, which is then the same, is simply handled in a different manner.

4.3 Implementation

In the procedure described in this section (see the flow diagram shown in Fig. 6), we denote by Ω the set of identified outliers. At the beginning of this procedure, Ω is therefore empty: $\Omega := \Omega_\phi \cup \Omega_p = \emptyset$. For simplicity, we now restrict ourselves to the limit case defined in Sect. 1.4.2). We then set

$$|w|_{\max} = \max_{j_\psi \notin \Omega} |w_{j_\psi}| \tag{68}$$

i.e. here: $|w|_{\max} = \max |w_{j_\psi}|$. Given some probability of false alarm θ_0, we define χ_0 as the upper $\theta_0/2$ probability point of the central normal distribution: $\chi_0 := N_{\theta_0/2}(0,1)$. For example, when θ_0 is equal to 0.001, χ_0 is of the order of 3.

1. Entrance local test

From Eqs. (59), (42) and (35), w is a reduced quantity. According to Eq. (39), in the absence of any bias, $|w|_{\max}$ must therefore be smaller than χ_0. In other terms, if $|w|_{\max} < \chi_0$, no outlier is to be searched: one then goes to step *4*. Conversely, if $|w|_{\max}$ is very large compared to χ_0 (say larger than 1000 for example), the QR process is to be reinitialized (see Sect. 3). In the other cases, the DIA procedure is initialized by setting $\mathfrak{r} = 1$ and $\Pi = \emptyset$; $\mathfrak{r}$ is a recursive index; the meaning of the auxillary set Π is defined in step *2.2* as soon as it begins to be built. At this stage, in the single-frequency case and in FLS mode (for example), the local redundancy is given by the formula $m = 2(n-1) - 3$.

2. Recursive identification of the outliers

2.1. Current set of potential outliers

Given some nonnegative constant $\kappa \leq 1$, form the current set of potential outliers (see Fig. 5):

$$\Pi_{\mathfrak{r}} := \left\{ j_\psi \notin \Omega : |w_{j_\psi}| \geq \kappa |w|_{\max} \right\}$$

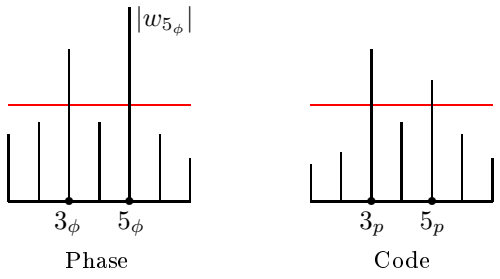

Fig. 5 *Notion of potential outliers in reduced mode.* The quantities $|w_{j_\psi}|$ shown here (in single-frequency mode) are the absolute values of the components of the (updated) residual w (see step *2.7*). In this illustration, $n = 7$, $\kappa = 0.5$ and $\Omega = \emptyset$; four potential outliers are identified: 3_ϕ, 5_ϕ, 3_p and 5_p. Here, the phase outlier 5_ϕ is likely to be the dominant potential outlier (see step *2.3*).

2.2. For each potential outlier $j_\psi \in \Pi_{\mathfrak{r}}$

Perform the following successive operations:

a) When $j_\psi \notin \Pi$, compute (see the context of Eqs. (64), (65), (61), (42) & (59) and Sect. 3.3)

$$f_{j_\psi} := H \cdot \left| \begin{array}{ll} z_{j_\phi} & \text{if } \psi = \phi \\ z_{j_p} & \text{if } \psi = p \end{array} \right.$$

Then, set

$$g_{j_\psi} := f_{j_\psi} \qquad \Pi \overset{\text{set}}{=} \left\{ \begin{array}{ll} \{j_\psi\} & \text{if } \Pi = \emptyset \\ \Pi \cup \{j_\psi\} & \text{otherwise} \end{array} \right.$$

By construction, Π is the set of potential outliers j_ψ for which f_{j_ψ} has already been computed.

b) If $\mathfrak{r} = 1$ go to step *2.2c*. Otherwise, at this level, $\{g^\circ_{\mathfrak{q}}\}_{\mathfrak{q}<\mathfrak{r}}$ is an orthonormal set. (This set is built, progressively, via step *2.4*.) Then, for each integer $\mathfrak{q} < \mathfrak{r}$, consider the inner product defined as follows:

$$\begin{aligned} \varsigma_{\mathfrak{q},j_\psi} &:= (g^\circ_{\mathfrak{q}} \cdot g_{j_\psi}) \\ &:= \sum_{\psi'=\phi,p} (g^\circ_{\mathfrak{q};\psi'} \cdot g_{j_\psi;\psi'}) \end{aligned}$$

This sum includes two terms. Depending on what ψ' refers to (ϕ or p), $g^\circ_{\mathfrak{q};\psi'}$ denotes the phase or code component of $g^\circ_{\mathfrak{q}}$, and likewise for $g_{j_\psi;\psi'}$. If $\varsigma_{\mathfrak{q},j_\psi}$ has not been computed yet, compute it, store it in memory, and perform the Gram-Schmidt orthogonalization operation

$$g_{j_\psi} \overset{\text{set}}{=} g_{j_\psi} - \varsigma_{\mathfrak{q},j_\psi} g^\circ_{\mathfrak{q}}$$

By construction, $\varsigma_{\mathfrak{q},j_\psi} = (g^\circ_{\mathfrak{q}} \cdot f_{j_\psi})$. At the end of all these operations, g_{j_ψ} is orthogonal to $g^\circ_{\mathfrak{q}}$ for any $\mathfrak{q} < \mathfrak{r}$.

c) Consider the projection of w on the one-dimensional space generated by g_{j_ψ}, i.e., $(h_{j_\psi} \cdot w) h_{j_\psi}$ where $h_{j_\psi} := g_{j_\psi} / \|g_{j_\psi}\|$. The norm of this projection is equal to $|(h_{j_\psi} \cdot w)|$, the absolute value of the quantity

$$\gamma_{j_\psi} := (g_{j_\psi} \cdot w) / \varrho_{j_\psi} \qquad \varrho_{j_\psi} := \|g_{j_\psi}\|$$

Explicitly,

$$\begin{aligned} (g_{j_\psi} \cdot w) &:= \sum_{\psi'=\phi,p} (g_{j_\psi;\psi'} \cdot w_{\psi'}) \\ \|g_{j_\psi}\|^2 &:= \sum_{\psi'=\phi,p} \|g_{j_\psi;\psi'}\|^2 \end{aligned}$$

2.3. Dominant potential outlier

The identified outlier $\bar{\jmath}_{\bar{\psi}}$ is defined as the dominant potential outlier, i.e., the potential outlier for which $|\gamma_{j_\psi}|$ is maximal:

$$\bar{\jmath}_{\bar{\psi}} := \underset{j_\psi \in \Pi_{\mathfrak{r}}}{\arg\max} |\gamma_{j_\psi}|$$

We then set

$$\omega_{\mathfrak{r}} := \bar{\jmath}_{\bar{\psi}} \qquad \Omega \overset{\text{set}}{=} \left\{ \begin{array}{ll} \{\omega_{\mathfrak{r}}\} & \text{if } \mathfrak{r} = 1 \\ \Omega \cup \{\omega_{\mathfrak{r}}\} & \text{if } \mathfrak{r} > 1 \end{array} \right.$$

$$\gamma^\circ_{\mathfrak{r}} := \gamma_{\omega_{\mathfrak{r}}} \qquad g^\circ_{\mathfrak{r}} := g_{\omega_{\mathfrak{r}}} / \varrho_{\omega_{\mathfrak{r}}}$$

Superscript $\circ$ stands for omega (and outlier). At this level, Ω is the current set of identified outliers:

$$\Omega = \{\omega_{\mathfrak{q}}\}_{\mathfrak{q}=1}^{\mathfrak{r}}$$

By construction, $\{g^\circ_{\mathfrak{q}}\}_{\mathfrak{q}=1}^{\mathfrak{r}}$ is an orthonormal basis of the current range of M; $\sum_{\mathfrak{q}=1}^{\mathfrak{r}} \gamma^\circ_{\mathfrak{q}} g^\circ_{\mathfrak{q}}$ is the projection of w on this space. With regard to Eq. (66), we then set

$$\beta^\circ_{\mathfrak{r}} := \beta_{\omega_{\mathfrak{r}}} \qquad f^\circ_{\mathfrak{r}} := f_{\omega_{\mathfrak{r}}}$$

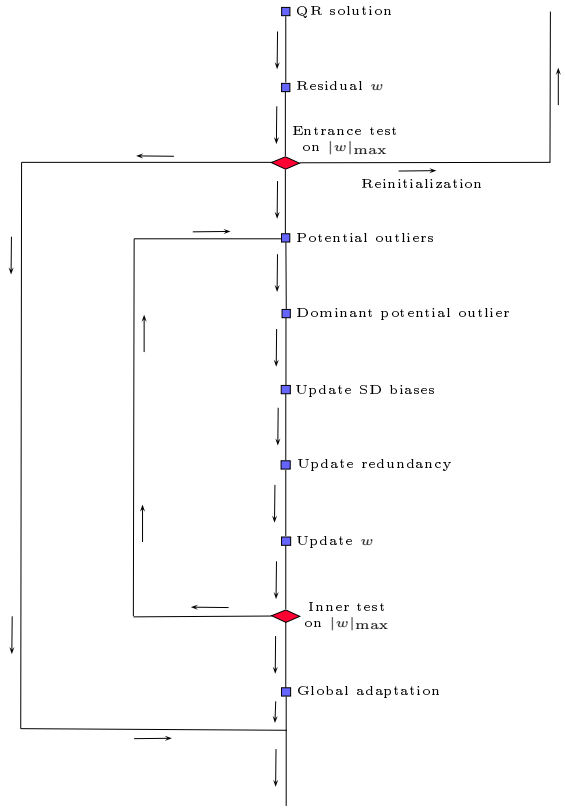

Fig. 6 *Flow diagram of the DIA procedure in reduced mode.* At each step of the identification process, the (updated) residual w is analyzed on the grounds of Eq. (68): see steps *1*, *2.7* and *2.8*. This allows the potential outliers to be selected (see Fig. 5). The outliers can thus be identified, in a recursive manner, via a particular orthogonalization Gram-Schmidt process. This QR Gram-Schmidt process also provides the SD biases, and thereby the cycle slips if any. When the ambiguity are not fixed, these biases are slightly refined through the global adaptation process described in Sect. 4.2.

2.4. Components of $g_{\mathfrak{r}}^{\circ}$ in the basis of the $f_{\mathfrak{q}}^{\circ}$'s

These components are denoted by $\mathrm{u}_{\mathfrak{q},\mathfrak{r}}$:

$$g_{\mathfrak{r}}^{\circ} = \sum_{\mathfrak{q}=1}^{\mathfrak{r}} \mathrm{u}_{\mathfrak{q},\mathfrak{r}} f_{\mathfrak{q}}^{\circ}$$

They are computed via the QR Gram-Schmidt formulas (see, e.g., Björck 1996)

$$\mathrm{u}_{\mathfrak{q},\mathfrak{r}} = \begin{cases} -\dfrac{1}{\varrho_{\omega_{\mathfrak{r}}}} \displaystyle\sum_{\mathfrak{q}\le\mathfrak{q}'<\mathfrak{r}} \mathrm{u}_{\mathfrak{q},\mathfrak{q}'}\, \varsigma_{\mathfrak{q}',\omega_{\mathfrak{r}}} & \text{if } \mathfrak{q}<\mathfrak{r} \\ \dfrac{1}{\varrho_{\omega_{\mathfrak{r}}}} & \text{if } \mathfrak{q}=\mathfrak{r} \end{cases}$$

for $1 \le \mathfrak{q} \le \mathfrak{r}$. The $\mathrm{u}_{\mathfrak{q},\mathfrak{r}}$'s are the entries of the $\mathfrak{r}^{\text{th}}$ column of an upper triangular matrix U.

2.5. Update the SD biases

According to Eq. (66), the SD biases $\beta_{\mathfrak{q}}^{\circ}$ are the components of $\sum_{\mathfrak{q}=1}^{\mathfrak{r}} \gamma_{\mathfrak{q}}^{\circ} g_{\mathfrak{q}}^{\circ}$ in the basis of the $f_{\mathfrak{q}}^{\circ}$'s:

$$\sum_{\mathfrak{q}=1}^{\mathfrak{r}} \gamma_{\mathfrak{q}}^{\circ} g_{\mathfrak{q}}^{\circ} = \sum_{\mathfrak{q}=1}^{\mathfrak{r}} \beta_{\mathfrak{q}}^{\circ} f_{\mathfrak{q}}^{\circ}$$

Denoting by $[\gamma^{\circ}]$ the column matrix with entries $\gamma_{\mathfrak{q}}^{\circ}$ (from $\mathfrak{q}=1$ to $\mathfrak{r}$), and likewise for $[\beta^{\circ}]$, we have

$$[\beta^{\circ}] = \mathrm{U}[\gamma^{\circ}]$$

The SD biases are therefore to be updated as follows:

$$\beta_{\mathfrak{q}}^{\circ} \overset{\text{set}}{=} \begin{cases} \beta_{\mathfrak{q}}^{\circ} + \mathrm{u}_{\mathfrak{q},\mathfrak{r}} \gamma_{\mathfrak{r}}^{\circ} & \text{if } \mathfrak{q}<\mathfrak{r} \\ \mathrm{u}_{\mathfrak{r},\mathfrak{r}} \gamma_{\mathfrak{r}}^{\circ} & \text{if } \mathfrak{q}=\mathfrak{r} \end{cases} \qquad (\text{for } 1 \le \mathfrak{q} \le \mathfrak{r})$$

2.6. Update the local redundancy

$$m \overset{\text{set}}{=} m-1$$

If $m=0$ go to step *3*.

2.7. Update w and $|w|_{\max}$

$$w \overset{\text{set}}{=} w - \gamma_{\mathfrak{r}}^{\circ} g_{\mathfrak{r}}^{\circ} \qquad |w|_{\max} \overset{\text{set}}{=} \max_{j_\psi \notin \Omega} |w_{j_\psi}|$$

2.8. Inner local test

If $|w|_{\max} > \chi_0$, update the recursive index: $\mathfrak{r} \overset{\text{set}}{=} \mathfrak{r}+1$. Then, go to step *2*.

3. Global adaptation

Update the global QR recursive process by taking account of the identified bias variables (see Sect. 4.2).

4. End

5 Examples

The QR implementation presented in this paper was validated by processing two GPS-data sets in dual-frequency mode (L1-C/A, L2-P). Shortly, these sets correspond to the following cases:

- **Static case.** Static reference receiver; static user receiver; 4907 epochs at 1 Hz; baseline size of the order of 250 m.
- **Kinematic case.** Static reference receiver; mobile user's car receiver; 973 epochs at 2 Hz; maximal baseline size of the order of 850 m.

The static case was studied to check our programs. In both cases, the standard deviations $\sigma_{\boldsymbol{\phi}}$ and $\sigma_{\boldsymbol{p}}$ were of the order of 3 mm and 55 cm, respectively (see Eq. (36)).

The reduced data were therefore centralized differences of type (39) with $\eta_j = 2$ for all j; χ_0 was set equal to 3. These data were processed in forced RLS mode (with initializations in LS mode).

As illustrated in Eq. (43), the float ambiguities were put in reverse order. Furthermore, to benefit from the analysis presented in Sects. 3.4 and 3.5, the L1 and L2 ambiguities were interwoven, as well as the L1 and L2 data in their phase and code column submatrices.

The optimal and suboptimal ambiguity solutions, $\dot{v}$ and $\dot{\dot{v}}$ respectively, were obtained (at each RLS epoch) by solving the nearest-lattice point problem defined in Sect. 3.6. It was thus possible to control the value of the 'global ambiguity-resolution parameter'

$$\varrho_1 := \frac{\|\dot{v} - \hat{v}\|^2_{V_{\hat{v}}^{-1}}}{\|\dot{\dot{v}} - \hat{v}\|^2_{V_{\hat{v}}^{-1}}} \tag{69}$$

The 'local ambiguity-resolution parameter'

$$\varrho_2 := \frac{|\dot{w}|_{\max}}{|\dot{\dot{w}}|_{\max}} \tag{70}$$

was also computed. Here, $\dot{w}$ and $\dot{\dot{w}}$ denote the values of the optimal and suboptimal residuals, respectively; note that the bias variables are then included in the local variable u_i. When

$$\varrho_1 \lesssim 0.5 \quad \text{or} \quad \varrho_2 \lesssim 0.4 \quad \text{(validation criterion)} \tag{71}$$

the ambiguities can be regarded as fixed.

All the programs were written in C language, including the LLL algorithm and the nearest-lattice point section. The first data set of 4907 epochs was thus processed, with $\kappa = 0$, in about five seconds on a standard personal computer. With $\kappa = 1$, this CPU time was reduced to three seconds with exactly the same results. The second data set of 973 epochs was processed in about two seconds for $\kappa = 0$, and in about one second for $\kappa = 1$.

5.1 Static case

In this case, due to major data-frame problems, the process was reinitialized at the following epochs: 1301, 3010 and 4689. As specified below for the first run, the ambiguities were fixed immediately. The position of the user receiver was thus retrieved, up to one or two centimeters, except for the initialization epochs of the four runs to be considered: 1, 1301, 3010 and 4689 (see Fig. 7).

We now concentrate on the first run. Seven or eight satellites were then visible: satellites 2, 5, 7, 8, 9, 23, 26 and sometimes 21. The latter appears and disappears (in an alternate manner) at the following epochs: 365, 878, 883, 884, 887, 888, 892, 896, 911, 936, 1004, 1098, 1130.

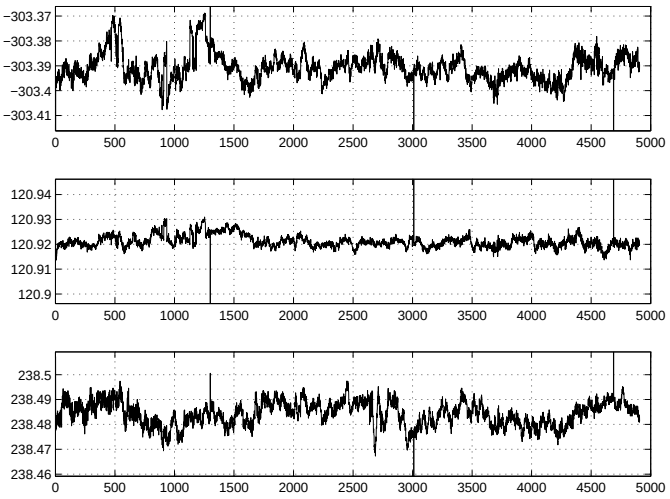

Fig. 7 *Static case (4907 epochs).* Relative coordinates (expressed in meters) of the user and reference receivers in the Earth-centred Earth-fixed (ECEF) frame: x, y, z (from the top to the bottom); see text and Fig. 8.

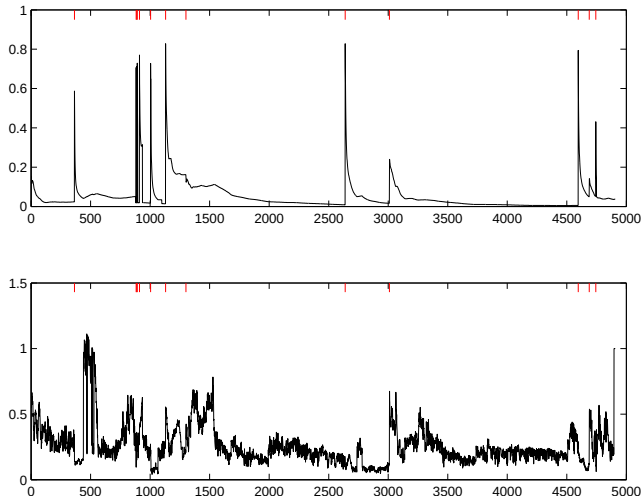

Fig. 8 *Static case (4907 epochs).* Ambiguity resolution parameters ϱ_1 (at the top) and ϱ_2 (at the bottom); see the context of Eqs. (69) to (71). The ambiguities are fixed, except at the initialization epoch 1 and at the reinitialization epochs 1301, 3010 and 4689 (see Fig. 7 and the corresponding red ticks). The other red ticks correspond to the epochs where a new satellite appears or reappears.

At epoch 1 (in LS mode), a code bias was identified on satellite 2 at frequency f_1; see steps *2.4* and *2.5* in Sect. 4.3. Its value, 7.02 m, was of course the same as that found by the adaptation process; see Sect. 4.2 and Fig. 6. The data of epoch 2 were of course processed in RLS mode. Again, a code bias was identified on satellite 2. As expected, its value, 6.70 m, was very close to that provided by the global adaptation process: 6.77 m. The ambiguities proved then to be fixed (see Table 1): ϱ_1 was smaller than 0.16 with ϱ_2 smaller than 0.65 (see Fig. 8 and Eqs. (69) to (71)). The code bias thus found was 5.42 m. Here, $|\dot{w}|_{\max} = 3.22$ and $|\dot{\dot{w}}|_{\max} = 5.07$.

Table 1: *Static case. Dual-frequency DD ambiguities.* The ambiguities shown here were fixed at epoch 2, just after the initialization epoch (see text).

satellite	f_1	f_2
2	0	0
5	995 532	783 561
7	1 585 927	329 961
8	−1 542 232	−893 259
9	13 115 987	10 232 032
23	6 934 437	4 872 157
26	10 017 404	7 778 866

As soon as satellite 21 appeared (at epoch 365), the corresponding ambiguities were immediately fixed:

satellite	f_1	f_2
21	−1 632 504	−777 230

At epoch 1093, large phase biases were identified on the L2 and L1 SD phase data of that satellite: 0.143 m and 0.107 m, respectively. As shown by the results obtained at the next epoch, these biases announced effective cycle slips. Indeed, at epoch 1094, one cycle slip was identified on the L2 SD phase of satellite 21, and likewise for the L1 SD phase of that satellite. More precisely, the biases identified by the RLS DIA procedure were then the following:

$$\begin{aligned}\beta_{f_2,21_\phi} &= \ \ 0.227\,\mathrm{m} \simeq \lambda_2\\ \beta_{f_1,21_\phi} &= \ \ 0.195\,\mathrm{m} \simeq \lambda_1\\ \beta_{f_1,21_p} &= -4.861\,\mathrm{m}\\ \beta_{f_2,21_p} &= \ \ 3.974\,\mathrm{m}\end{aligned}$$

At that epoch, the entrance value of $|w|_{\max}$ was large compare to $3 : 28.40$. The outliers were then identified as specified below:

Outlier	$\lvert w\rvert_{\max}$
$(f_2\,;21_\phi)$	29.64
$(f_1\,;21_\phi)$	5.49
$(f_1\,;21_p)$	4.49
$(f_2\,;21_p)$	2.30

Here, the value in the right-hand side column is the corresponding residual value of $|w|_{\max}$. Corrected from the cycles slips thus identified, the data were then processed without any large phase biases until the disappearance of satellite 21 at epoch 1098, and then without any difficulty until the major data-frame problem at epoch 1301.

In the second run, from epoch 1301 to epoch 2060 included, all the previous 8 satellites were visible. The reference satellite s_1 (satellite 2) then disappeared at epoch 2061. A similar situation occured in the fourth run with nine satellites: the reference satellite s_1 (satellite 1 in that run) disappeared at epoch 4743. To check the section of the program corresponding to the disappearance of other satellites in RLS mode (see Sect. 3.5), the SD data of satellite s_2 (then satellite 5) were discarded at epoch 4775. As expected, the corresponding results were correct.

From epoch 4897 to the end of the fourth run, the optimal and suboptimal sets of L1 ambiguities coincide up to an integer constant: the unity for all j; the optimal and suboptimal sets of L2 ambiguities are then identical. As at those epochs, the reference satellite is not visible, the reduced values of $\dot{v}$ and $\dot{\dot{v}}$ are the same (see Eq. (53) and Eqs. (39) & (40) with $\eta_j = 2$ for all j). It then follows that $\dot{w} = \dot{\dot{w}}$, hence $\varrho_2 = 1$ (see Fig. 8). The ambiguities are however fixed. Indeed ϱ_1 is then less than 0.04 (see Eq. (71)).

5.2 Kinematic case

In this case, nine to eleven satellites were visible: satellites 4, 9, 16, 18, 19, 22, 23, 24, 28, 29 and 32. The ambiguities were immediately fixed with ϱ_1 less than 0.15 and ϱ_2 less than 0.33 (see Table 2 and Figs. 9 & 10; satellite 9 was not then visible).

Table 2: *Kinematic case. Dual-frequency DD ambiguities.* The ambiguities shown here were fixed at epoch 2, just after the initialization epoch (see text).

satellite	f_1	f_2
4	0	0
16	−577 343	−425 713
18	−489 386	−357 110
19	16 040	40 057
22	187 137	178 615
23	−611 408	−448 519
24	−188 663	−122 172
28	−1 651 396	−1 238 734
29	363 726	308 953
32	−19 687	2 051

A major data problem appeared at epoch 222. The process was then reinitialized by the RLS DIA procedure. Indeed, the entrance value of $|w|_{\max}$ was greater than 10^6 (see step *1* in Sect. 4.3). The ambiguities were then fixed again, but only eleven seconds later (after epoch 244; see Fig. 10 and Eq. (71)).

Just to show the efficiency of our approach, cycles slips were imposed at epoch 960: −1 cycle in the reception of the f_1-signal coming from the reference satellite; 2 cycles in the reception of the f_2-signal coming from satellite 23; 1 cycle in the reception of the f_2-signal coming from satellite 29.

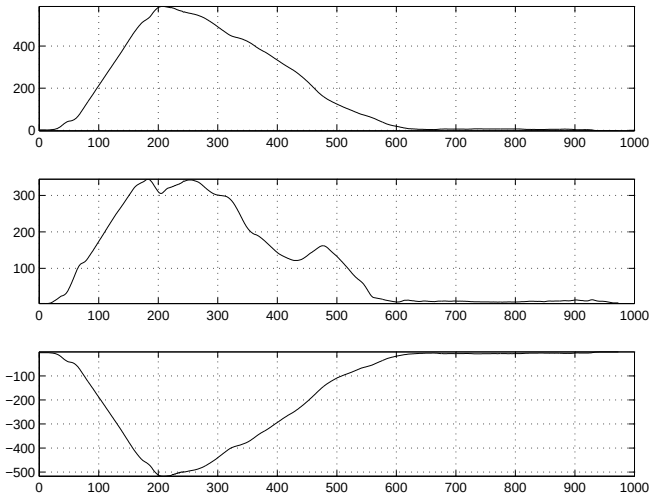

Fig. 9 *Kinematic case (973 epochs).* Relative positions (in meters) of the user and reference receivers in the ECEF frame: x, y, z (from the top to the bottom); see text and Fig. 10.

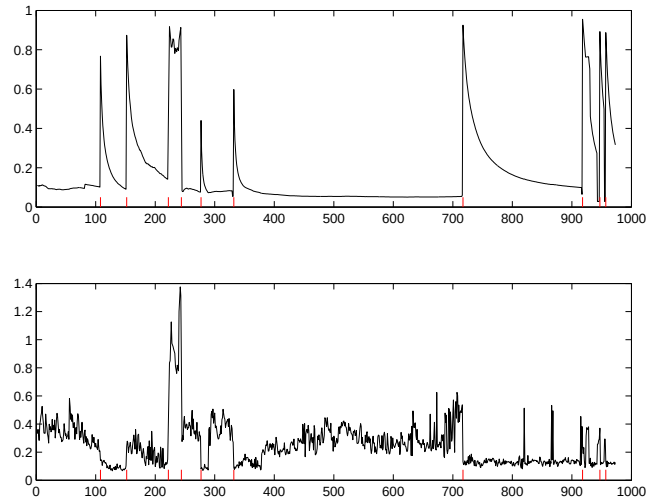

Fig. 10 *Kinematic situation (973 epochs).* Ambiguity resolution parameters ϱ_1 (at the top) and ϱ_2 (at the bottom); see the context of Eqs. (69) to (71). The ambiguities are fixed, except at the initialization epoch and from epochs 222 to 244 included (see text and the corresponding red ticks). The other red ticks correspond to the epochs where a new satellite appears or reappears.

At that epoch, the entrance value of $|w|_{\max}$ was then of the order of 69. In the RLS DIA procedure, the outliers were then identified as follows:

Outlier	$\lvert w\rvert_{\max}$
$(f_2\,;23_\phi)$	46.57
$(f_2\,;29_\phi)$	29.06
$(f_1, 4_\phi)$	2.66

The SD biases finally obtained by the process were then the following:

$$\begin{aligned}\beta_{f_2,23_\phi} &= \quad 0.488\,\mathrm{m} \;\simeq 2\lambda_2\\ \beta_{f_2\,;29_\phi} &= \quad 0.239\,\mathrm{m} \;\simeq \lambda_2\\ \beta_{f_1\,;\;4_\phi} &= -0.196\,\mathrm{m} \;\simeq -\lambda_1\end{aligned}$$

Corrected from the cycles slips thus identified, the data were processed without any difficulty until the end of the run (epoch 973).

6 Concluding comments

As clarified in Sect. 1.4, the notions of reduction and centralization correspond to the same concept. The variance-covariance matrix of the reduced or centralized data is the identity. For example, in the single-baseline case, the reference formulas are Eqs. (39) and (40). In the centralized approaches, the QR method can therefore be applied directly. This not the case in the usual DD approach. Indeed, the Cholesky factorization of the inverse of the variance-covariance matrix of the DD data must then be performed. Moreover, in the centralized approaches, all the SD data are handled in the same manner. The corresponding numerical codes are therefore more readable than those of their DD versions.

The QR implementation of GNSS centralized approaches is also well suited to quality control. The search for the potential outliers is performed by simple inspection of the absolute value of the components of the successive updated residuals (see Fig. 5 and step *2.7* in Sect. 4.3). The statistical tests are thereby very simple (see steps *1* and *2.8* in Sect. 4.3). Moreover, as the Givens rotations of the QR recursive processes can easily be stored in memory, the variational calculations involved in the DIA method can be performed in a very efficient manner; see Sect. 3.3 and step *2.2* in Sect. 4.3. Furthermore, the QR global adaptation step of the DIA method nicely completes the QR Gram-Schmidt step *2.4* of the local identification process described in Sect. 4.3. The SD biases, among which the cycles slips (if any), are thus determined in two different ways.

For simplicity, the study presented in this paper was restricted to the case of RTK observations with a single baseline of local scale. The extension to multiple-baseline networks with possibly missing data follows the guidelines of the present contribution. The main points to be developed concern the following topics:

- Handling the integer ambiguities;
- Reduction of the undifferential optimization problem (equivalent of Sect. 1.4 for the undifferential data);
- QR solution of the reduced optimization problem;
- Integer-ambiguity resolution;
- Identifiable biases;
- Related DIA method.

References

Agrell E., Eriksson T., Vardy A. and Zeger K. (2002) ***Closest point search in lattices***. IEEE Trans. Inform. Theory. 48: 2201–2214.

Bierman G.J. (1977) ***Factorization methods for discrete sequential estimation***, Vol. 128 in Mathematics in science and engineering, Academic Press, Inc. New-York.

Björck A. (1996) ***Numerical methods for least-squares problems***, SIAM.

Chang X.-W. and Guo Y. (2005) ***Huber's estimation in relative GPS positioning: computational aspects***. J. Geod. 79: 351–362.

Feng Y. and Li B. (2008) ***Three-carrier ambiguity resolution: generalized problems, models, methods and performance analysis using semi-generated triple frequency GPS data***. Proc. ION GNSS-2008. Savannah, Georgia USA: 2831-2840

Golub G.H. and van Loan C.F. (1989) ***Matrix computations***, second edition, The Johns Hopkins University Press, Baltimore, Maryland.

Hewitson S., Lee H.K. and Wang J. (2004) ***Localizability analysis for GPS/Galileo receiver autonomous integrity monitoring***. The Journal of Navigation, Royal Institute of Navigation 57: 245–259.

Lannes A. (2007a) ***On the concept of reduced difference in differential GNSS***. C. R. Mécanique. 335: 720–726.

Lannes A. (2007b) ***Differential GPS: the reduced difference approach***. J. GPS. 6: 23–37.

Lannes A. (2008) ***GNSS networks with missing data: identifiable biases and potential outliers***. Proc. ENC GNSS-2008. Toulouse, France: 1–11.

Liu X. (2002) ***A comparison of stochastic models for GPS single differential kinematic positioning***. Proc. ION GPS-2002. Portland, Oregon USA: 1830-1841.

Loehnert E., Wolf R., Pielmeier J., Werner W. and Zink T. (2000) ***Concepts and performance results on the combination of different integrity methods using UAIM and GNSS without SA***. Proc. ION GPSS-2000. Salt Lake City, Utah USA: 2831-2840

Luk F.T. and Tracy D.M. (2008) ***An improved LLL algorithm***. Linear algebra and its applications. 428: 441–452.

Shi P. H. and Han S. (1992) ***Centralized undifferential method for GPS network adjustment***. Australian Journal of Geodesy, Photogrammetry and Surveying. 57: 89-100.

Strang G. and Borre K. (1997) ***Linear algebra, geodesy, and GPS***, Wellesley-Cambridge Press, Massachussets.

Teunissen P.J.G. (1990) ***An integrity and quality control procedure for use in multi sensor integration***. Proc. ION GPS-90. Colorado Springs, Colorado USA: 513-522

Tiberius C.C.J.M. (1998) ***Recursive data processing for kinematic GPS surveying***, Publications on Geodesy, New series: ISSN 0165 1706, Number 45, Netherlands Geodetic Commission, Delft.

Xu P. (2001) ***Random simulation and GPS decorrelation***. J. Geod. 75: 408–423.